

## Ultrasonic Measurement of Minute Displacement of Object Cyclically Actuated by Acoustic Radiation Force

Kazuaki MICHISHITA, Hideyuki HASEGAWA and Hiroshi KANAI\*

Graduate School of Engineering, Tohoku University, Sendai 980-8579, Japan

(Received November 18, 2002; accepted for publication March 12, 2003)

Recently, several researchers have investigated the potential of the use of acoustic radiation force for imaging the mechanical properties of tissue. However, these methods have some problems as to safety and the spatial resolution. Therefore, an alternative ultrasonic remote actuation and measurement method is proposed in this paper, in which the intensity of the applied continuous ultrasonic wave is suppressed to be lower than the safety guideline ( $1 \text{ W/cm}^2$ ) recommended by the Japan Society of Ultrasonics in Medicine (JSUM). A minute displacement with amplitude of less than  $1 \mu\text{m}$  is cyclically generated by the radiation force with a low frequency  $\Delta f$  of several hertz. For simultaneous measurement of the minute displacement, cyclic radiation force is applied intermittently by maintaining its envelope waveform of the low-frequency component of  $\Delta f \text{ Hz}$ . At the same time, an ultrasonic correlation-based method, namely, the *phased tracking method*, is employed to measure the minute displacement. In basic experiments, the minute displacement of several micrometers was generated in silicone rubber by applying radiation force, and it was successfully measured by the *phased tracking method*.

[DOI: 10.1143/JJAP.42.4608]

KEYWORDS: acoustic radiation force, noninvasive measurement, measurement of minute displacement, viscoelasticity measurement, tissue characterization

### 1. Introduction

In recent years, some remote actuation methods based on acoustic radiation force have been reported. Fatemi and coworkers proposed an imaging method called ultrasound-stimulated acoustic emission (USA-E).<sup>1,2)</sup> Their system consists of two confocal ultrasonic transducers, and two ultrasound beams with two slightly different frequencies  $f$  and  $(f + \Delta f)$  are transmitted. Acoustic radiation pressure  $P_R(t)$  exerted on the interface between different media is a function of the energy density,  $e(t)$ , and the specific acoustic impedances,  $Z_1$  and  $Z_2$ , of the medium.<sup>3)</sup> The energy density,  $e(t)$ , is proportional to the square of the sum of the sound pressures,  $p_1(t)$  and  $p_2(t)$ , generated by the two transducers. In the intersectional area of the two beams, therefore, an oscillatory radiation pressure  $P_R(t)$  with the frequency difference,  $\Delta f$ , is applied to the interface. The radiation force produces acoustic emission which is closely related to the mechanical frequency response of the medium. By measuring the acoustic emission with a hydrophone, hard inclusions in a soft material were experimentally detected. However, the spatial resolution in the depth direction corresponds to the size of the intersectional area.

Nightingale *et al.* proposed an alternative imaging method in which the focused ultrasound is employed for applying the radiation force to a soft tissue during short durations (less than 1 ms). The viscoelastic properties of the tissue are investigated from the magnitude and the transient response of the displacement,  $d(t)$ , of the tissue.<sup>4)</sup> In order to generate measurable displacement,  $d(t)$ , using several ultrasonic pulses, high-intensity pulsed ultrasound of  $1,000 \text{ W/cm}^2$  is employed. According to the safety guideline shown by JSUM, however, the intensity of ultrasound is recommended to be less than  $240 \text{ mW/cm}^2$  and  $1 \text{ W/cm}^2$ , for the pulsed wave and the continuous wave, respectively.<sup>5)</sup> Therefore, the intensity of the pulsed ultrasound employed by Nightingale *et al.* is far greater than that indicated in the safety guideline.

In this study, in order to apply ultrasound within the range of the safety guideline and to detect the minute displacement,  $d(t)$ , generated by the resultant acoustic radiation force, the two continuous-wave (CW) ultrasound beams of  $f$  and  $f + \Delta f$  are employed to cyclically actuate the acoustic radiation pressure at low frequency ( $\Delta f$ ) to increase the signal-to-noise ratio. For the measurement of the resultant minute displacements, an ultrasound correlation-based method, the *phased tracking method*,<sup>6)</sup> is employed. By sweeping the low frequency  $\Delta f$ , the frequency characteristics of the object are determined. Moreover, from the amplitude characteristics of the displacement,  $d(t)$ , continuously generated by the acoustic radiation pressure,  $P_R(t)$ , the viscoelasticity of the object can be determined. We constructed an experimental setup and confirmed the measurement of the minute cyclic displacement by the *phased tracking method* using several micrometers.

### 2. Principle

When continuous plane-wave ultrasound is incident on an interface between two different media, as illustrated in Fig. 1, a constant force, which is called an acoustic radiation force, is exerted on the interface. Acoustic radiation pressure,  $P_R(t)$ , is defined as the radiation force per unit area of the object, as follows:

$$P_R(t) = (1 + R^2)\langle e(t) \rangle, \quad (2.1)$$

where  $R$  and  $\langle e(t) \rangle$  are the reflection coefficient of sound pressure and the temporally averaged energy density at the

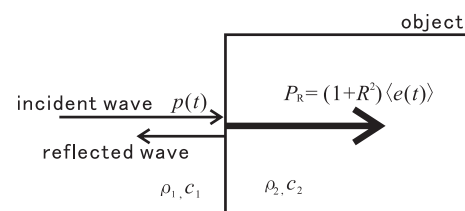


Fig. 1. The acoustic pressure  $p(t)$  of the incident wave exerts the acoustic radiation pressure,  $P_R(t)$ , on an object.

\*E-mail address: hkanai@ecei.tohoku.ac.jp

interface, respectively. In eq. (2.1), the incident wave through the interface is assumed to be perfectly absorbed into the object. Using the density,  $\rho_1$  and  $\rho_2$ , and sound speed,  $c_1$  and  $c_2$ , of each medium, the reflection coefficient,  $R$ , and temporally averaged energy density,  $\langle e(t) \rangle$ , are defined by

$$R = \frac{Z_2 - Z_1}{Z_2 + Z_1} = \frac{\rho_2 c_2 - \rho_1 c_1}{\rho_2 c_2 + \rho_1 c_1}, \quad (2.2)$$

$$\langle e(t) \rangle = \frac{1}{\rho_1 c_1^2} \frac{1}{T} \int_0^T \{p(t)\}^2 dt, \quad (2.3)$$

where  $p(t)$  is the sound pressure at the interface and  $T$  is the averaging period. JSUM shows the safety guideline, in which the intensity of the CW ultrasound should be less than  $1 \text{ W/cm}^2$ . By assuming that density  $\rho_1$  and sound speed  $c_1$  of water are  $10^3 \text{ kg/m}^3$  and  $1,500 \text{ m/s}$ , respectively, the acoustic radiation pressure,  $P_R(t)$ , exerted on the interface of the totally absorbing object is calculated as  $6.67 \text{ Pa}$  when the ultrasound intensity is  $1 \text{ W/cm}^2$ .

The energy density,  $e(t)$ , of the incident wave is proportional to the square of the sound pressure  $p(t)$  of the ultrasound beam. When two ultrasonic beams with slightly different frequencies,  $f$  and  $f + \Delta f$ , cross each other, the sound pressure,  $p_{\text{sum}}(t)$ , at the interface is expressed by the sum of sound pressure of two ultrasonic beams as follows:

$$p_{\text{sum}}(t) = p_0 \cos \omega t + p_0 \cos(\omega + \Delta\omega)t, \quad (2.4)$$

where  $p_0$ ,  $\omega$ , and  $\Delta\omega$ , are the amplitude of the sound pressure  $p(t)$  of each ultrasound beam, angular frequency of the incident wave ( $\omega = 2\pi f$ ), and difference in angular frequency ( $\Delta\omega = 2\pi\Delta f$ ), respectively. For this case, the energy density  $e(t)$  is expressed by

$$\begin{aligned} e(t) &= \frac{1}{\rho_1 c_1^2} \{p_{\text{sum}}(t)\}^2 \\ &= \frac{1}{\rho_1 c_1^2} \{p_0 \cos \omega t + p_0 \cos(\omega + \Delta\omega)t\}^2 \\ &= \frac{p_0^2}{\rho_1 c_1^2} \left\{ 1 + \cos \Delta\omega t + \cos(2\omega + \Delta\omega)t \right. \\ &\quad \left. + \frac{1}{2} \cos 2\omega t + \frac{1}{2} \cos 2(\omega + \Delta\omega)t \right\}. \end{aligned} \quad (2.5)$$

From the second term of the right-hand side of eq. (2.5), it is found that the energy density  $e(t)$  of the incident field has a component with the frequency difference  $\Delta f$ . Therefore, the cyclically oscillatory radiation pressure,  $P_R(t)$ , at the frequency difference  $\Delta f$  of eq. (2.1) is given by

$$P_R(t) = (1 + R^2) \frac{p_0^2}{\rho_1 c_1^2} \cos \Delta\omega t. \quad (2.6)$$

Thus, using the two crossed ultrasound beams at the slightly different frequencies,  $f$  and  $f + \Delta f$ , the oscillatory radiation force can be cyclically applied to the intersectional area of the beams. The amplitude and phase characteristics of the displacement,  $d(t)$ , which is generated as a response to the radiation force, relate to the viscoelasticity of the target. By sweeping the frequency difference  $\Delta f$  and detecting the

displacements  $d(t)$  generated by the radiation force, the viscoelasticity of the object can be characterized.

### 3. Experimental Setup

An experimental setup is shown in Fig. 2. In order to measure the displacement,  $d(t)$ , we employed ultrasonic diagnostic equipment (Toshiba SSH-160A) with a sector array probe (center frequency: 5 MHz). The equipment was modified to detect the minute displacement  $d(t)$  of an object by the *phased tracking method*. The object ( $45 \times 40 \times 10 \text{ mm}$  silicone rubber; static elastic modulus  $E_S$  was measured as  $20 \text{ kPa}$ ) was placed at the bottom of a water tank, and the ultrasonic probe was fixed  $5 \text{ cm}$  away from the object. For the application of radiation pressure,  $P_R(t)$ , an ultrasonic transducer (Tokimec 5Z10I, center frequency: 5 MHz) was driven by a sum of two CWs with two slightly different frequencies ( $5 \text{ MHz}$  and  $5 \text{ MHz} + \Delta f$ ) generated by a function generator (Sony Tektronix AFG2020).

When CW ultrasound is employed for actuation, interference occurs between the CW ultrasound for actuation and the pulsed ultrasound for displacement measurement. In order to avoid this interference, it is necessary to stop actuation during transmission and reception of this ultrasonic pulse for measurement. Therefore, we made an electrical switch to control the cessation of the CW ultrasound for actuation. Figure 3 shows a time chart for actuation and measurement. Only for actuation period (A) when the control signal in Fig. 3(b) was turned on, did the electrical switch pass the signals for actuation. Then, the signal was amplified and the ultrasound for actuation was transmitted from the transducer during period (A). It is necessary to set the length of period (A) so that the successively transmitted

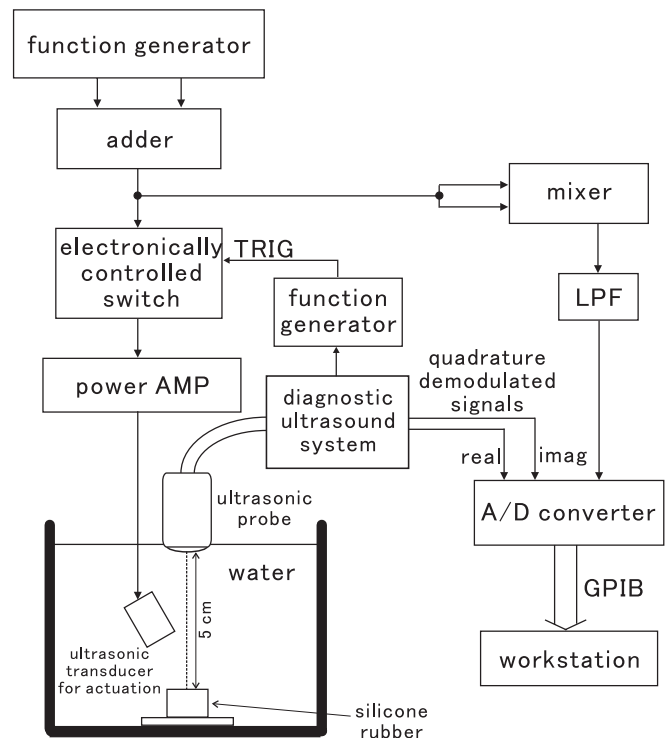


Fig. 2. Experimental setup for measurement of the displacement of an object cyclically actuated by ultrasound.

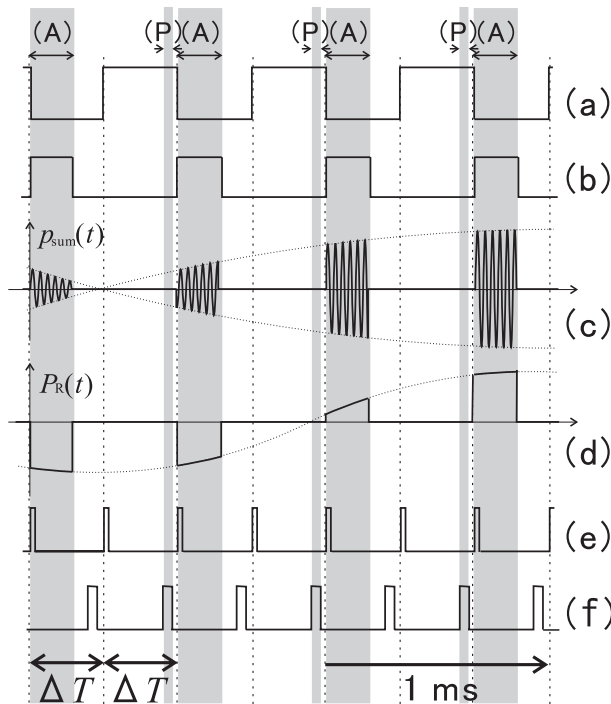


Fig. 3. Time chart for actuation and measurement. (a) Timing clock from the diagnostic scanner. (b) Period (A) of actuation controlled by the electrical switch. (c) The sound pressure,  $p_{\text{sum}}(t)$ , consisting of the sum of two ultrasound beams with slightly different frequencies,  $f$  and  $f + \Delta f$ , applied intermittently only during actuation period (A). (d) The acoustic radiation pressure,  $P_R(t)$ , generated by the sound pressure in Fig. 3(c). (e) Timing of the transmission of the ultrasonic pulse for measurement from the probe. (f) The sampling gate of the RF echo data in probe period (P).

measurement pulse is prevented from interfering with reverberations of the ultrasound for actuation. Therefore, as shown in Fig. 3(c), the ultrasound for actuation was transmitted intermittently, and then the radiation pressure  $P_R(t)$  became a series of pulses whose envelope consisted of the sinusoidal wave with the frequency difference  $\Delta f$ , as shown in Fig. 3(d).

At the rising edge of the trigger pulse in Fig. 3(e), on the other hand, an ultrasonic pulse was transmitted from the ultrasonic probe in Fig. 2. In order to track the displacement  $d(t)$  of the object, the quadrature-demodulated signals of the RF echo data were A/D converted during the gates shown in Fig. 3(f). In order to avoid interference between the ultrasound for actuation and that for measurement, the data which were stored in the periods other than probe period (P) were not used for the measurement of the displacement  $d(t)$  of the object.

#### 4. Experimental Results

Figure 4(a) shows the M-mode image of the object. In Fig. 4, the difference frequency  $\Delta f = 7$  Hz was employed. Acoustic radiation pressure,  $P_R(t)$ , shown in Fig. 4(b) was calculated based on eq. (2.6) as follows: The density,  $\rho_2$ , and the sound speed,  $c_2$ , of the object were measured as  $0.98 \times 10^3$  kg/m<sup>3</sup> and  $1.0 \times 10^3$  m/s, respectively, in a separate experiment. By assuming the density,  $\rho_1$ , and the sound speed,  $c_1$ , of water to be  $1.0 \times 10^3$  kg/m<sup>3</sup> and  $1.5 \times 10^3$  m/s, respectively, the pressure reflection coefficient,  $R$ , and the energy reflection coefficient,  $R^2$ , were respectively calculated as  $-0.21$  and  $0.044$  using eq. (2.2).

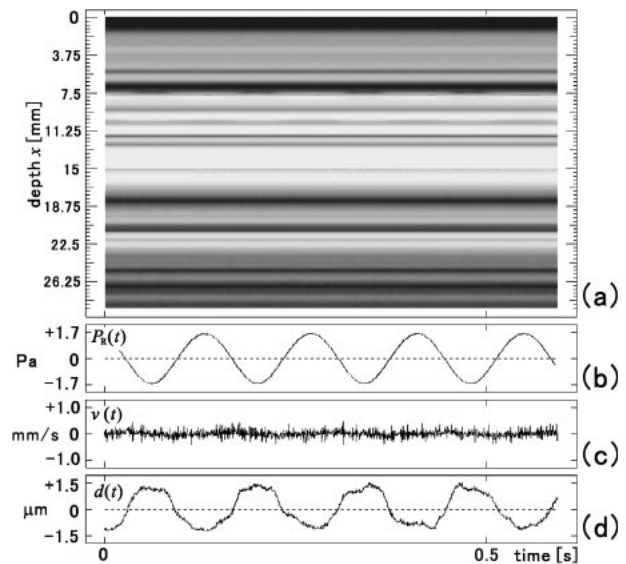


Fig. 4. The results of the experiment with the frequency difference  $\Delta f = 7$  Hz. (a) M-mode image of the object. The black line at the depth of  $x = 7.725$  mm shows the tracked displacement. (b) The estimated acoustic radiation pressure,  $P_R(t)$ , given by eq. (2.6). (c) The vibration velocity of the object,  $v_A(t)$ , obtained by the *phased tracking method*. (d) The displacement of the object,  $d(t)$ .

By measuring the acoustic field of the ultrasound for actuation with a hydrophone (Force Institute, MH-28-10), the amplitude of the spatially averaged sound pressure,  $p_0$ , was obtained beforehand and plotted as a function of the voltage applied to the transducer, as shown in Fig. 5. In this study, the amplitude of the applied voltage,  $V_0$ , was 32 V. Therefore, by neglecting the attenuation of the medium surrounding the object, the component of the sound pressure,  $p_0$ , which is perpendicular to the interface of the object, was calculated as 61 kPa.

The absorption coefficient of the object was also measured beforehand. Figure 6(a) shows the measurement system used. The ultrasonic transducer was driven by a sum of two CWs with slightly different frequencies (5 MHz and 5 MHz + 10 Hz, the amplitude of the applied voltage,  $V_0$ , for each CW: 30 V). The sound pressure,  $p_0$ , of the ultrasound was measured with the hydrophone which was fixed at 5 cm away from the transducer. As shown in Fig. 6(b), in the case of interposing the object between the transducer and the hydrophone, the measured sound pressure,  $p_1(t)$ , was

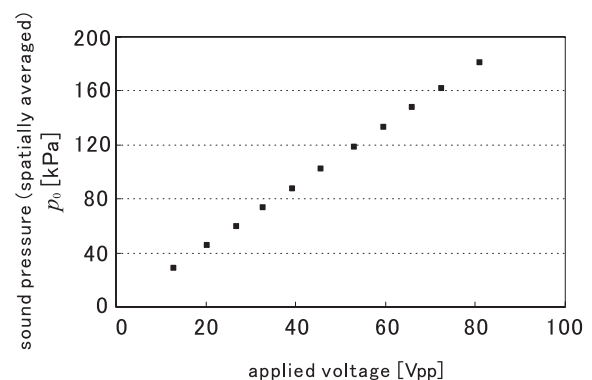


Fig. 5. Spatially averaged sound pressure  $p_0$  transmitted from the transducer as a function of the voltage applied to the transducer.

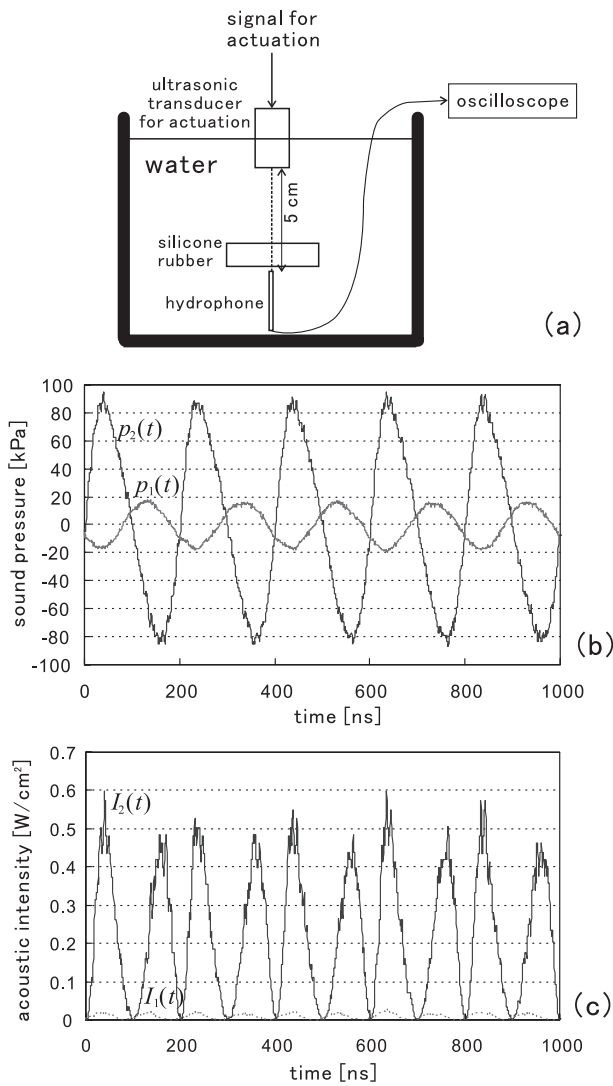


Fig. 6. (a) The experimental setup for measurement of the absorption coefficient of the object. (b) The sound pressure,  $p_1(t)$ , was measured using a hydrophone with the object interposed between the transducer and the hydrophone. The sound pressure,  $p_2(t)$ , was measured without the object. (c) Ultrasonic intensities,  $I_1(t)$  and  $I_2(t)$ , calculated from  $p_1(t)$  and  $p_2(t)$ , respectively.

smaller than that,  $p_2(t)$ , without the object due to attenuation by the object. Figure 6(c) shows the ultrasonic intensities,  $I_1(t)$  and  $I_2(t)$ , calculated from sound pressures,  $p_1(t)$  and  $p_2(t)$ , respectively. Temporally averaged intensities of  $I_1(t)$  and  $I_2(t)$  were calculated as  $0.23 \text{ W/cm}^2$  and  $8.8 \times 10^{-3} \text{ W/cm}^2$ , respectively. The absorption coefficient,  $\alpha$ , is defined by the ratio of the transparent intensity,  $I_2(t)$ , to the incident intensity,  $I_1(t)$ . Thus, the absorption coefficient,  $\alpha$ , was calculated as 0.038. Since the acoustic intensity was attenuated by about 96% by the object, the object can be assumed to be a totally absorbing material.

From these results, by assuming the object to be a totally absorbing material ( $R = 0$ ), the acoustic radiation pressure,  $P_R(t)$ , exerted on the interface of the object was calculated as 1.7 Pa, using eq. (2.6) as shown in Fig. 4(b).

The vibration velocity,  $v(t)$ , of the object actuated by the acoustic radiation force was measured by the *phased tracking method*, as shown in Fig. 4(c). By integrating the velocity  $v(t)$ , the displacement of the object,  $d(t)$ , was

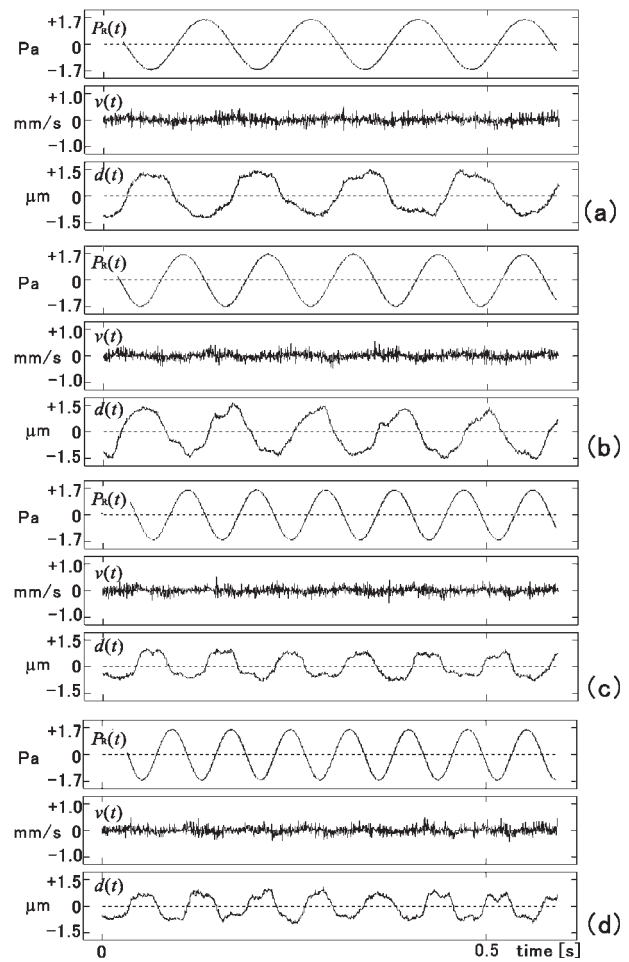


Fig. 7. For each frequency difference  $\Delta f$ , three experimental results are shown: the estimated acoustic radiation pressure  $P_R(t)$  given by eq. (2.6), the vibration velocity  $v(t)$  of the object measured by the *phased tracking method*, and the displacement  $d(t)$  of the object. (a)  $\Delta f = 7 \text{ Hz}$ . (b)  $\Delta f = 9 \text{ Hz}$ . (c)  $\Delta f = 11 \text{ Hz}$ . (d)  $\Delta f = 13 \text{ Hz}$ .

obtained as shown in Fig. 4(d). In Fig. 4(d), it is seen that the object was cyclically actuated at the frequency difference,  $\Delta f$ , of 7 Hz with an amplitude of the order of a few micrometers.

For the frequency difference,  $\Delta f$ , swept from 7 Hz to 13 Hz, the results are shown in Fig. 7. For each  $\Delta f$ , an almost cyclic component with  $\Delta f$  can be found in the measured displacement.

By assuming the Voigt model to be a viscoelastic model of the object, the absolute value of the complex elastic modulus,  $|E^*|$ , of the object is given by

$$|E^*| = |E_S + j\Delta\omega\eta| = \frac{P_{R\max}}{\frac{d_{\max}}{d_0}}, \quad (4.1)$$

where  $P_{R\max}$  and  $d_{\max}$  are the amplitude of the radiation pressure  $P_R(t)$  and that of the change in thickness from the the initial thickness,  $d_0$ , of the object ( $d_0 = 10 \text{ mm}$ ), respectively.  $E_S$  and  $\eta$  are the static elastic modulus and the viscosity coefficient, respectively.

In Fig. 8, the absolute value of the complex elastic modulus,  $|E^*|$ , of the object is plotted as a function of the frequency difference,  $\Delta f$ . Circles and diamonds show the results measured by the proposed method and using the laser

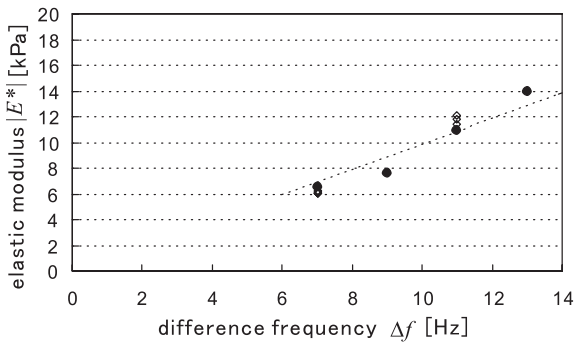


Fig. 8. The absolute value of the complex elastic modulus,  $|E^*|$ , of the object as a function of the frequency difference  $\Delta f$ , obtained by eq. (4.1). Circles and diamonds show the results measured by the proposed method and using the laser Doppler velocimeter, respectively.

Doppler velocimeter, respectively. In eq. (4.1), the absolute value of the complex elastic modulus,  $|E^*|$ , gradually increases with the frequency difference,  $\Delta f$ , which reflects the viscoelastic properties of the object.

## 5. Conclusion

In this study, we constructed an experimental setup for cyclic remote actuation of the object and showed the

measurement results of minute displacements,  $d(t)$ , in the micrometer order actuated by the acoustic radiation pressure,  $P_R(t)$ , by using the *phased tracking method*. A single transducer was driven by the sum of the two continuous waves having slightly different frequencies,  $f$  and  $f + \Delta f$ . The duration of the ultrasound for remote actuation was controlled to prevent ultrasonic displacement measurement from the interference. The frequency characteristics of the absolute value of the complex elastic modulus  $|E^*|$  calculated from the resultant displacement,  $d(t)$ , generated by the radiation pressure,  $P_R(t)$ , showed the viscoelastic properties of the object. From these results, it was shown that the proposed method has the potential to accurately measure the viscoelasticity of a regional area of the object.

- 1) M. Fatemi, L. E. Wold, A. Alizad and J. F. Greenleaf: IEEE Trans. Med. Imag. **21** (2002) 1.
- 2) M. Fatemi and J. F. Greenleaf: Proc. Natl. Acad. Sci. USA **96** (1999) 6603.
- 3) G. R. Torr: Am. J. Phys. **52** (1984) 402.
- 4) K. Nightingale, M. S. Soo, R. Nightingale and G. Trahey: Ultrasound Med. Biol. **28** (2002) 227.
- 5) JSUM: Jpn. J. Med. Ultrason. **11** (1984) 41 [in Japanese].
- 6) H. Kanai, M. Sato, Y. Koiwa and N. Chubachi: IEEE Trans. UFFC **43** (1996) 791.